NEURAL REGENERATION RESEARCH
Volume 8, Issue 16, June 2013

www.nrronline.org

doi:10.3969/j.issn.1673-5374.2013.16.002 [http://www.nrronline.org; http://www.sjzsyj.org]
Zhou JH, Sui FG, Yao M, Wang YS, Liu YG, Tian FP, Li Q, He XF, Shao L, Liu ZQ. Novel nanometer scaffolds regulate the biological behaviors of neural stem cells. Neural Regen Res. 2013;8(16):1455-1464.

Novel nanometer scaffolds regulate the biological behaviors of neural stem cells☆

Jihui Zhou[1], Fuge Sui[1], Meng Yao[2], Yansong Wang[2], Yugang Liu[2], Feipeng Tian[1], Qiang Li[1], Xiaofeng He[1], Lin Shao[1], Zhiqiang Liu[1]

1 *Longnan Hospital of Daqing, i.e. the Fifth Hospital Affiliated to Qiqihar Medical University, Daqing 163453, Heilongjiang Province, China*
2 *Department of Spine Surgery, the Second Hospital Affiliated to Harbin Medical University, Harbin 150086, Heilongjiang Province, China*

Abstract

Ideal tissue-engineered scaffold materials regulate proliferation, apoptosis and differentiation of cells seeded on them by regulating gene expression. In this study, aligned and randomly oriented collagen nanofiber scaffolds were prepared using electronic spinning technology. Their diameters and appearance reached the standards of tissue-engineered nanometer scaffolds. The nanofiber scaffolds were characterized by a high swelling ratio, high porosity and good mechanical properties. The proliferation of spinal cord-derived neural stem cells on novel nanofiber scaffolds was obviously enhanced. The proportions of cells in the S and G_2/M phases noticeably increased. Moreover, the proliferation rate of neural stem cells on the aligned collagen nanofiber scaffolds was high. The expression levels of cyclin D1 and cyclin-dependent kinase 2 were increased. Bcl-2 expression was significantly increased, but Bax and caspase-3 gene expressions were obviously decreased. There was no significant difference in the differentiation of neural stem cells into neurons on aligned and randomly oriented collagen nanofiber scaffolds. These results indicate that novel nanofiber scaffolds could promote the proliferation of spinal cord-derived neural stem cells and inhibit apoptosis without inducing differentiation. Nanofiber scaffolds regulate apoptosis and proliferation in neural stem cells by altering gene expression.

Key Words

neural regeneration; stem cells; tissue engineering; spinal cord-derived neural stem cells; nanofiber scaffolds; proliferation; apoptosis; differentiation; neuroregeneration

Research Highlights

(1) Electronic spinning technology was used to obtain randomly oriented nanofiber membranes and aligned nanofiber membranes. The aligned and randomly oriented collagen nanometer scaffolds were shown to alter the biological behaviors of neural stem cells and induce changes in gene expression.
(2) The effects of the aligned nanofiber membranes on promoting neural stem cell proliferation and on inhibiting apoptosis of neural stem cells were better than those of the randomly oriented nanofiber membranes. Aligned and randomly oriented collagen nanometer scaffolds did not significantly induce apoptosis or differentiation in stem cells.
(3) Aligned and randomly oriented collagen nanometer scaffolds regulated the expression of apoptosis and cell cycle genes in neural stem cells.

Jihui Zhou☆, M.D., Associate chief physician.

Jihui Zhou and Fuge Sui contributed equally to this article.

Corresponding author: Meng Yao, Ph.D., Professor, Department of Spine Surgery, the Second Hospital Affiliated to Harbin Medical University, Harbin 150086, Heilongjiang Province, China, doctoryaomeng@163.com. Yansong Wang, Ph.D., Associate professor, Master's supervisor, Department of Spine Surgery, the Second Hospital Affiliated to Harbin Medical University, Harbin 150086, Heilongjiang Province, China, wys1975@163.com.

Received: 2013-02-04
Accepted: 2013-05-06
(N20120608002)

INTRODUCTION

Scaffolds created using nanotechnology have beneficial effects on the biological behaviors of cells seeded on their surfaces, *e.g*., differentiation, proliferation and apoptosis. The performance of scaffolds is very important for the reparative properties of cells grown on them, and nanotechnology has shown promise for spinal cord tissue engineering[1-2]. Current research is mainly focused on two areas: (1) the surface characteristics of scaffolds made by nanotechnology are more similar to the three-dimensional topological structure of the extracellular matrix and thus the performance is improved, the histocompatibility is better and the effects on the biological behaviors of cells are more beneficial. (2) Scaffolds may also be used as vectors for genes and drugs to promote the differentiation and proliferation of cells, and to improve their reparative properties[3-7]. Electronic spinning technology has become the main method for manufacturing nanofiber scaffolds, instead of phase separation and self-assembly. Electronic spinning technology enables simple control of the fiber orientation and diameter. Electronic spinning nanofiber scaffolds have high porosity, good plasticity and are similar to the three-dimensional topological structure of the extracellular matrix. Such better performance may affect the biological behaviors of seeded cells, *e.g*., adhesion, differentiation, proliferation and apoptosis[8]. Electronic spinning technology has improved the manufacturing technology, and is suitable for core-shell type scaffolds or scaffolds made of new raw materials. Scaffolds made using electronic spinning technology may also be used as vectors for genes and drugs[9]. Most extracellular matrices are three-dimensional topological structures composed of nanoscale collagen. Collagen is an ideal tissue-engineered scaffold material. The surface of nanofiber scaffolds prepared by the electrospinning technique is very similar to the extracellular matrix[10].

Neural stem cells have potential to migrate and differentiate into multiple cell types, and are therefore ideal for spinal cord tissue engineering. An ideal scaffold material may affect cell proliferation, apoptosis and differentiation by regulating gene expression. This study was designed to test the performance of spinal cord tissue-engineered nanometer scaffolds made of the collagen using electronic spinning technology. The influences of the nanometer scaffolds on the proliferation, apoptosis and differentiation of spinal cord-derived neural stem cells were analyzed by flow cytometry. The changes in gene expression were analyzed by real-time quantitative PCR.

RESULTS

Properties of nanometer scaffolds

Scanning electron microscopy showed that the directions of the fibers in the aligned collagen nanometer scaffolds were generally similar. The diameter of the fibers, which was determined using a special image computing system (provided by Harbin Forestry University, China), was 694 ± 157 nm. The randomly oriented collagen fibers were criss-crossed and their diameter was 694 ± 157 nm (Figure 1). Both the porosity of the aligned collagen nanofiber scaffolds (79.31 ± 2.87%) and the porosity of randomly oriented nanofiber scaffolds (84.53 ± 1.65%) were over 70%. The swelling ratios of the randomly oriented and aligned collagen nanofiber scaffolds were 386.11 ± 1.32% and 334.30 ± 2.07%, respectively.

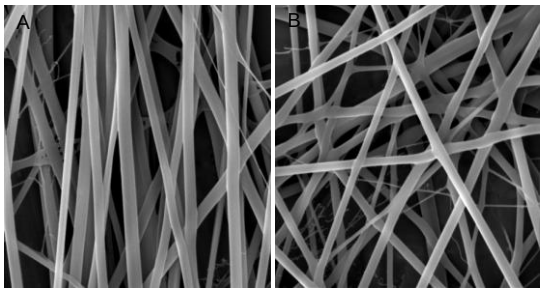

Figure 1 Characterization of aligned and randomly oriented collagen nanometer scaffolds (scanning electron microscopy, × 5 000).

(A) The directions of the fibers in aligned collagen nanometer scaffolds were generally similar. (B) The fibers in randomly oriented collagen were criss-crossed.

The tensile strength of the aligned collagen nanofibers was higher (30 MPa) than that of randomly oriented nanofibers (14.5 MPa) (at 0.2 mm thickness). These results were consistent with reports from others showing that the mechanical properties of nanofiber scaffolds are highly dependent on the orientation of the nanofibers (Table 1).

Culture and identification of neural stem cells

The cultured spinal cord-derived neural stem cells were spherical under the microscope. Most of the cells were suspended and were single on the first day of culture. The cell nuclei and cytoplasm were clearly distinguishable. A small amount of cells aggregated to form irregular masses. Cell debris and non-viable cells sunk to the bottom of the bottle, and a small amount of cells adhered to the bottle walls. Most of the cells were

still single on the second day, and the cells aggregated to form irregular large clumps, which were not neurospheres and could be aspirated off. The cells proliferated and formed neurospheres that were unequal in size following culture for 2–3 days. There were several cells initially, and the cell number gradually increased with time in culture. Most of the neurospheres were oval, suspended, and their boundaries were clear. Viable cells were observed in the center of neurospheres under a high-power microscope. Cell viability in the center of neurospheres decreased with increasing cell number. The number of cells in neurospheres increased to 100 or several hundred by the 7th day. Some neurospheres were large enough to be visible to the naked eye. Most of the neurospheres were suspended, and parts of large neurospheres attached to the bottle walls. Following mechanical passage, the cell proliferation rate was similar to that of primary cells (Figure 2).

Table 1 Properties of nanometer scaffolds

Index	Aligned collagen nanometer scaffold	Randomly oriented collagen nanometer scaffold
Porosity (%)	79.31±2.87	84.53±1.65
Swelling ratio (%)	386.11±1.32	334.30±2.07
Elastic modulus (MPa)	1.93±0.82	1.73±0.33
Tensile strength (MPa)	31.02±3.22	14.64±3.23
Elongation at break (%)	5.90±0.85	5.23±3.04

Swelling ratio (%) = $(W_1–W_0)/W_0 \times 100\%$. W_0 is the sample initial quality; W_1 is the sample wet mass. The average value was applied. Mechanical properties were determined using an Instron 3365 uniaxial tensile machine. Data are represented as mean ± SD.

Double immunofluorescence staining showed that the cultured spinal cord cells were neural progenitor cells by the expression of nestin, a progenitor cell marker. The nestin-positive cells were also able to incorporate 5-bromo-2-deoxyuridine (BrdU) (Figure 3).

Good biocompatibility between tissue-engineered nanometer scaffolds and neural stem cells

The survival of neural progenitor cells was examined using the 3-(4,5-dimethylthiazol-2-yl)-5-(3-carboxymethoxyphenyl)-2-(4-sulfophenyl)-2H-tetrazolium (MTS) assay at 1, 3, 5, 7 and 9 days after seeding. On day 1, the cell numbers in the collagen nanofiber groups were significantly less than those in the control group ($P < 0.05$). From day 3 to day 9, the cell numbers in the collagen nanofiber groups were significantly greater than those in the control group ($P < 0.05$; Table 2). The cell numbers in the aligned group were significantly greater than those in the random group. At 7 and 9 days, the cell number appeared to reach a ceiling level in the three groups.

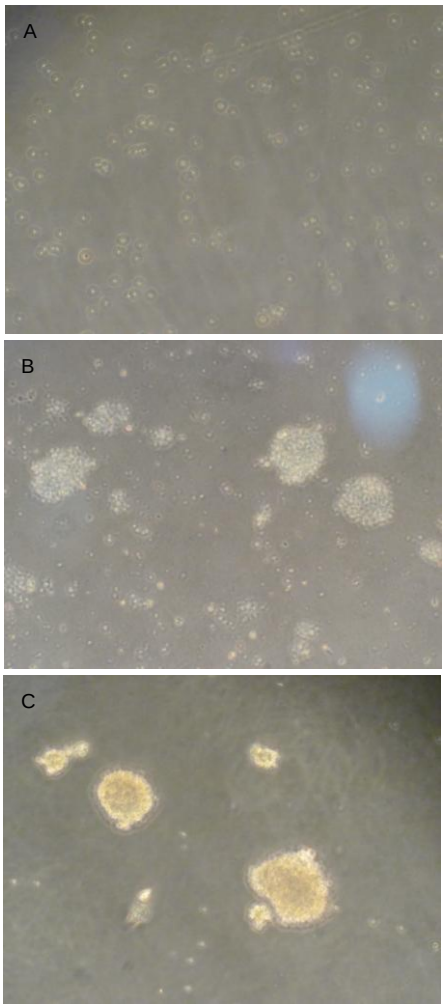

Figure 2 Morphology of cultured spinal cord-derived neural stem cells (inverted microscope, × 40).

(A) The cells grew in suspension and were spherical on the first day of primary culture.

(B) The cells had proliferated and formed neurospheres on the third day of primary culture.

(C) Some neurospheres were large enough to be visible to the naked eye and fibroblasts adhered to the bottle wall on the 7th day of primary culture.

Effects of tissue-engineered nanometer scaffolds on the proliferation and apoptosis of neural stem cells

The results of cell cycle analysis showed that the percentage of cells in the control group at S phase and G_2/M phase was 5.75 ± 1.7%. The percentage of cells in the aligned group at S phase and G_2/M phase was 11.8 ± 1.6%. The percentage of cells in the random group at S phase and G_2/M phase was 9.5 ± 1.4%. The percentage of S phase and G_2/M phase cells in the aligned group was obviously higher than that in the other two groups ($P < 0.05$). The percentage of S phase and G_2/M phase cells in the random group was obviously higher than that in the control group ($P < 0.05$).

Table 2 Effects of nanometer scaffolds on the survival rates (absorbance) of neural stem cells

Culture time (day)	Control group	Aligned group	Random group	*F*	*P*
1	0.24±0.09	0.32±0.01	0.35±0.01	143.03	< 0.05
3	0.43±0.02	0.71±0.02[ab]	0.58±0.01	349.04	< 0.05
5	0.70±0.02	0.87±0.02[ab]	0.70±0.02	101.65	< 0.05
7	0.80±0.02	0.97±0.01[ab]	0.89±0.01	160.91	< 0.05
9	0.89±0.01	0.94±0.01[ab]	0.92±0.02	37.44	< 0.05

The survival rates of neural stem cells were determined by 3-(4,5-dimethylthiazol-2-yl)-5-(3-carboxymethoxyphenyl)-2-(4-sulfophenyl)-2H-tetrazolium (MTS) assay. Data are represented as mean ± SD of eight wells in each group. Differences between groups were analyzed by one-way analysis of variance. [a]*P* < 0.05, *vs*. control group; [b]*P* < 0.05, *vs*. random group.

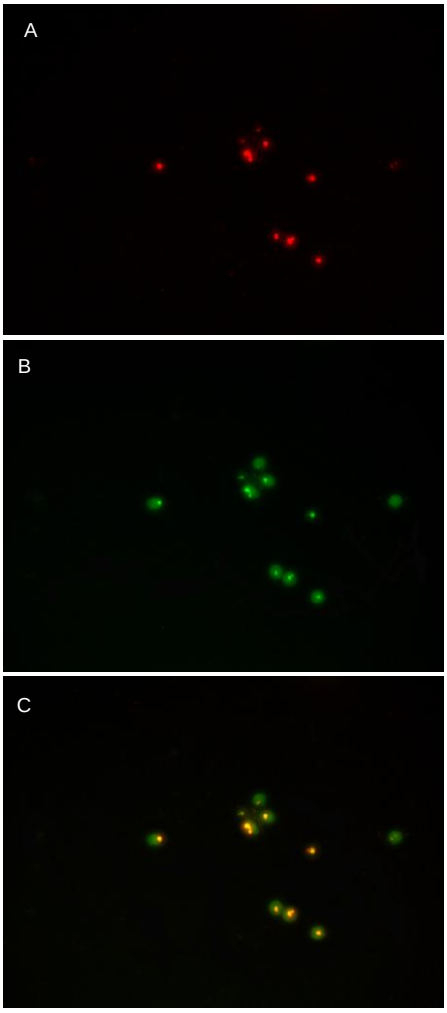

Figure 3 Cells at passage 2 expressed nestin and 5-bromo-2-deoxyuridine (BrdU) (double fluorescent immunohistochemistry, fluorescence microscopy, × 40).

(A) The cells expressed nestin and showed bright green fluorescence following labeling with rhodamine.

(B) The cells expressed BrdU and showed bright orange red fluorescence following labeling with fluorescein isothiocyanate.

(C) Merge of (A) and (B).

The rate of apoptosis in the aligned group was 8.89 ± 0.31%, which was much lower than that in the random group (9.27 ± 0.17%) and the control group (10.55 ± 0.33%) (*P* < 0.05). The rate of apoptosis in the random group was much lower than that in the control group (*P* < 0.05; Figure 4, Table 3).

Tissue-engineered nanometer scaffolds did not affect the differentiation of neural stem cells

The rates of differentiation into neurons were 12.47 ± 2.34% in the control group, 12.65 ± 2.20% in the aligned group, and 12.44 ± 2.51% in the random group (*P* > 0.05; Figure 5).

Expression of cell cycle and apoptosis genes in cells cultured on aligned and randomly oriented collagen nanofiber membranes

Real-time quantitative PCR revealed that the expression levels of the cell cycle genes, cyclin D1, cyclin-dependent kinase 2 and anti-apoptotic gene Bcl-2 were increased significantly in the aligned group and random group (*P* < 0.05). The levels of the three genes were increased significantly in the aligned group compared with the other groups (*P* < 0.05). The expression levels of pro-apoptotic genes, Bax and caspase-3, were decreased significantly in the aligned group and random group (*P* < 0.05). There was no significant difference in expression levels between the aligned and random groups (*P* > 0.05; Figure 6).

DISCUSSION

Collagen is a common component of extracellular matrices in animal tissues. It promotes cell proliferation and migration, and shows good biocompatibility. Collagen has become an effective scaffold material in spinal tissue engineering. However, its poor mechanical properties and other shortcomings must be overcome to improve its physicochemical and biological properties for practical applications.

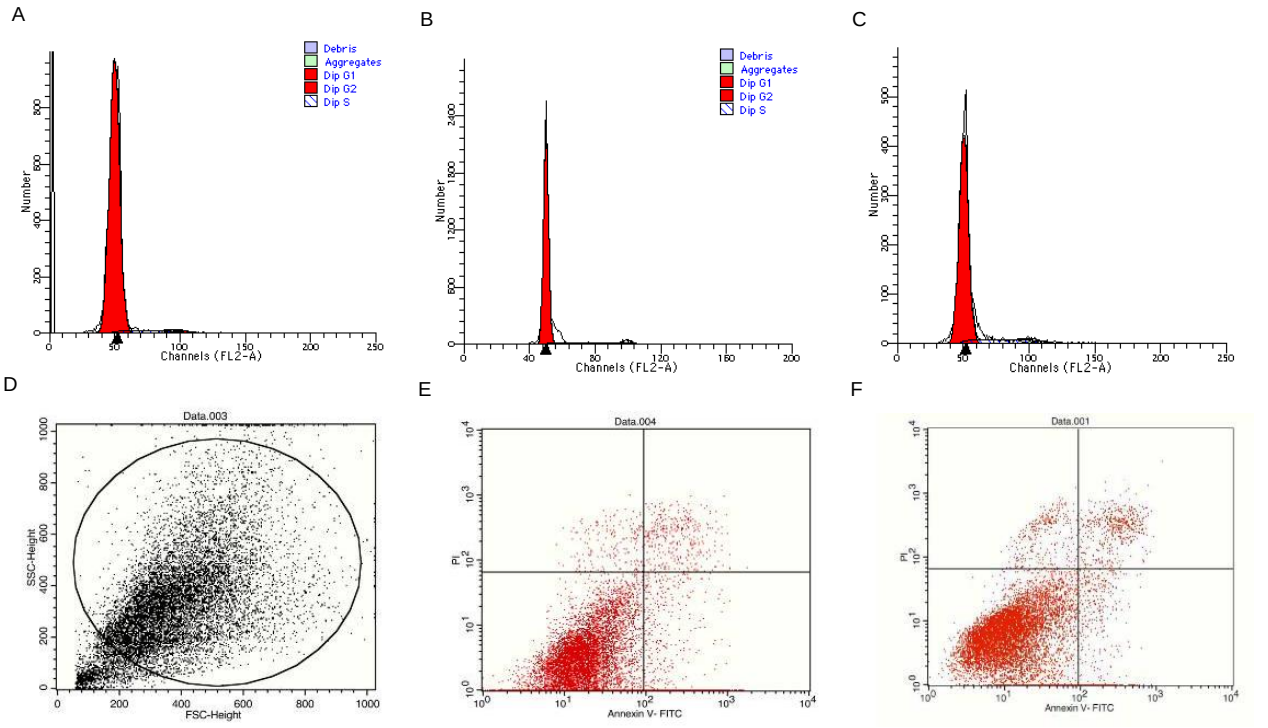

Figure 4 Effects of tissue-engineered nanometer scaffolds on cell cycle and apoptosis in neural stem cells as detected by flow cytometry.

The percentage of cells in the multiplication period in the aligned group (C) was obviously higher than that in the other two groups ($P < 0.05$). Results for the random group (B) were obviously higher than those for the control group (A) ($P < 0.05$).

The percentages of apoptotic cells in the aligned group (D, E) and random group were obviously lower than the percentage in the control group (F). The results for the aligned group and the random group were similar. (D) Cell column chart for the aligned group: the more concentrated the column, the higher the cell purity. (E, F) Graphs of apoptotic cells analyzed by flow cytometry: live cells are in the left lower quadrant; dead cells are in the left higher quadrant; early apoptotic cells are in the right higher quadrant; late apoptotic cells are in the right lower quadrant.

Table 3 Effects of nanometer scaffolds on cell proliferation and apoptosis

Group	Percentage of cells in the multiplication period (%)	Percentage of apoptotic cells (%)
Control	5.80±1.70	10.55±0.33
Aligned	11.80±1.60[ab]	8.89±0.31[a]
Random	9.50±1.40[a]	9.27±0.17[a]

Data are represented as mean ± SD. Differences between groups were analyzed by one-way analysis of variance. [a]$P < 0.05$, *vs*. control group; [b]$P < 0.05$, *vs*. random group.

With the rise and development of nanotechnology, the performance of collagen scaffolds is continually being improved[11-14].

In this study, electronic spinning technology was applied to make aligned and randomly oriented nanofiber scaffolds with type I collagen as the raw material. As expected, the direction of fibers in aligned nanofiber scaffolds was consistent, while the fibers in random nanofiber scaffolds were criss-crossed.

Tissue-engineered scaffolds can effectively fill tissue defects, prevent the development of scar tissue and provide nesting sites for seed cells and endogenous repair cells. An ideal scaffold should have the following properties[15]: good histocompatibility and almost no immune rejection; minimal local and systemic inflammatory responses; non-toxic to seed cells and adjacent tissue; high porosity and swelling ratio for cell material exchange; gradual degradation over a particular period of time to meet the needs of tissue regeneration; mechanical stability in the body; minimal effects on the biological behaviors of cells seeded on its surface. The results showed that the porosity and swelling ratio of aligned collagen nanofiber scaffolds and randomly oriented nanofiber scaffolds were high and satisfactory, indicating that their mechanical properties meet the needs of spinal cord repair.

The properties of the nanometer scaffolds were tested. The porosities of aligned collagen nanofiber scaffolds

and randomly oriented nanofiber scaffolds were both over 70%; high porosity increases the surface area of the nanofiber membrane, which is helpful for cell adhesion and proliferation. Their swelling ratio was also high, thus enabling them to be easily shaped for manufacturing scaffolds. The appropriate pore size together with high porosity may provide the cells with more space to grow.

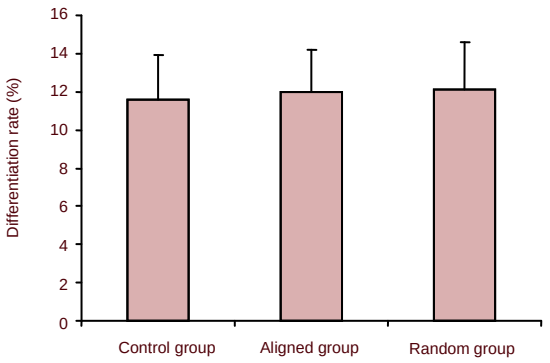

Figure 5 Effects of nanometer scaffolds on cell differentiation.

The microtubule-associated protein 2-positive cell rate was used to determine the differentiation rate of neural stem cells into neurons. Data are represented as mean ± SD. Tests were repeated four times. Differences between groups were analyzed by one-way analysis of variance.

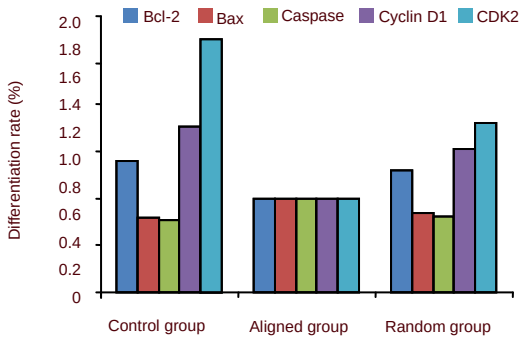

Figure 6 Changes in the expression of proliferation and apoptosis genes in cells cultured on aligned and randomly oriented collagen nanofiber membranes.

The relative amount of target gene expression = $2^{-\Delta\Delta t}$. $2^{-\Delta\Delta t}$ represents the difference in expression of target genes between the experimental group and the control group. Measurement data are represented as mean ± SD. Differences between groups were analyzed by one-way analysis of variance. $^{a}P < 0.05$, *vs*. control group; $^{b}P < 0.05$, *vs*. random group. CDK2: Cyclin-dependent kinase 2.

The elastic modulus, tensile strength and elongation at break were tested in the mechanical performance test. Elastic modulus represents the deformation resistance of the bracket and is inversely proportional to resistance to deformation of materials, *i.e*., the smaller the value, the stronger the resistance to deformation of the bracket. The elongation at break represents the elongation ratio of the material when it is broken, and it is also inversely proportional to resistance to deformation of materials. The tensile strength represents the greatest tensile force the material can bear before it is broken and it is proportional to the resistance to deformation of materials, *i.e.*, the greater the value, the stronger the resistance to deformation of the bracket. The elastic modulus of spinal cord tissue is 300 Pa[16-17]. The mechanical performance of the two nanofiber scaffolds was obviously better than the normal spinal cord, and their mechanical performance was better after swelling. The two nanofiber scaffolds have good properties and may be ideal scaffolds for spinal cord tissue engineering.

MTS reduction is an indicator of cell number and is used to examine cell survival in this study. Both aligned collagen nanofiber scaffolds and randomly oriented nanofiber scaffolds increased the survival rates of neural stem cells, and aligned collagen nanofiber scaffolds were more efficient.

Neural stem cell proliferation is controlled by cell cycle regulatory factors, including extracellular and intracellular factors. Cyclin-dependent kinase is the central regulatory factor, and its expression increases cell proliferation. Cell cycle proteins (cyclins) can promote the expression of cyclin-dependent kinase, and then enhance cell proliferation positively. Cyclin-dependent kinase inhibitor inhibits the expression of cyclin-dependent kinase, and thus inhibits cell proliferation. The three factors constitute the basis of cell cycle regulation[18], and the related genes coding the three factors are the key genes for the regulation of cell proliferation. In this research, aligned collagen nanofiber scaffolds and randomly oriented nanofiber scaffolds increased the expression of cyclin-dependent kinase and cyclin, and inhibited the expression of cyclin-dependent kinase inhibitor, thus promoting cell proliferation.

The occurrence and development of cell apoptosis are controlled by specific genes. When cells are subjected to apoptosis-inducing factors, pro-apoptotic genes are activated and apoptosis is induced. Cells also express anti-apoptotic genes, and there is a dynamic balance between anti-apoptotic genes and pro-apoptotic genes. For example, the Bax gene can promote apoptosis, while the Bcl-2 gene can inhibit apoptosis. Caspases can inactivate Bcl-2 and subsequently induce apoptosis[19-21].

In this study, aligned collagen nanofiber scaffolds and randomly oriented nanofiber scaffolds increased the expression of Bcl-2 and decreased the expression of Bax and caspase, thus inhibiting apoptosis.

The differentiation of neural stem cells into neurons is the research focus of many scholars, with the aim of regenerating the injured nervous system. The regulation of neural stem cell differentiation is controlled by regulatory factors and complex situations[22]. Aligned collagen nanofiber scaffold and randomly oriented nanofiber scaffolds were expected to increase neural stem cell differentiation into neurons by changing the cellular microenvironment, but the scaffolds did not alter endogenous regulatory factors.

MATERIALS AND METHODS

Design

A comparative observation of cell biology.

Time and setting

Experiments were performed in the Central Laboratory of the Second Hospital Affiliated to Harbin Medical University in China from March 2010 to September 2011.

Materials

A total of 50 Sprague-Dawley rats born within 24 hours, irrespective of gender, were purchased from the Animal Center of the Second Hospital Affiliated to Harbin Medical University in China, animal license No. SYXK (Hei) 2010-07. Animals were housed at 20–25°C and 45–50% humidity, and were breast fed. The protocols were conducted in accordance with the *Guidance Suggestions for the Care and Use of Laboratory Animals*, formulated by the Ministry of Science and Technology of China[23].

Methods

Preparation of aligned and random orientation nanofiber membranes

Type I collagen (Sigma-Aldrich, St. Louis, MO, USA) was dissolved in 1,1,1,3,3,3-hexafluoro-2-propanol (Sigma-Aldrich) at a concentration of 8% weight-per-volume. The composite solution was fed into a 5 mL plastic syringe fitted with a stainless steel blunt needle with a diameter at 0.5 mm. The positive lead from the high voltage supply was attached to the external surface of the metal syringe needle. At the onset of electrospinning, the infusion pump was set to deliver the composite solution at an injection rate of 0.5 mL/h. Simultaneously, a high voltage of 7 kV was applied to the composite solution. Randomly oriented collagen fibers were collected on a flat collector wrapped with aluminum foil at a distance of 10 cm from the needle tip. Aligned nanofibers were formed using a rotating drum with a diameter of 50 mm at a rate of 3 000 r/min. The scaffolds were dried overnight under vacuum at room temperature.

Testing the morphologies of the electrospun aligned and randomly oriented fiber membranes

The morphologies of the electrospun aligned and randomly oriented collagen fibers were characterized by scanning electron microscopy (CamScanMX2600FE, Oxford, UK). Nanofiber membranes were cut into chips with the diameter of about 2 mm, stuck onto the observation platform and numbered. The accelerating voltage was 24 kV. All samples were coated with a thin layer of platinum in two 30-second consecutive cycles at 45 mA. Scanning electron micrographs were analyzed with image analysis software provided by Harbin Forestry University, China. To calculate diameter and porosity, five images were selected, four fibers were selected randomly in each image and their diameters were measured, and then the average value was applied.

Mechanical properties of the electrospun aligned and randomly oriented fiber membranes

Aligned and randomly oriented fiber membranes were cut into strips of about 40 × 5 mm^2. Their mechanical properties were determined using an Instron 3365 uniaxial tensile machine (Model 3365, Instron, Norwood, MA, USA) with a 100 N load cell under a cross-head speed of 10 mm/min. Five samples were tested for each type of electrospun fibrous scaffold. The elastic modulus, tensile strength and elongation at break were tested.

Swelling ratios of the electrospun aligned and randomly oriented fiber membranes

The water absorption capacities of the scaffolds were determined from the swelling ratio[24]. Ten samples of the aligned and randomly oriented fiber membranes were separately selected, cut into rectangles, and immersed in deionized water for 12 hours. Excess water was absorbed with filter paper. The swelling ratio was calculated using the following formula: swelling ratio (%) = $(W_1–W_0)/W_0$ × 100%, where W_0 is initial quality and W_1 is wet mass. The average value was calculated.

Culture and identification of neural stem cells

Neonatal Sprague-Dawley rats born within 24 hours were immersed in ethanol for 10 minutes. The skin was cut open and the spine was removed. The spinal cord was

collected and placed into cold 0.01 mmol/L PBS. Spinal cord membrane and blood vessels were stripped completely and the spinal cord was cut into strips of 0.5–1 mm^3. The strips were filtered through a cell sieve with a 200 mesh to remove connective tissue and bulky tissue. The spinal cord was incubated in Hank's buffered saline solution supplemented with 0.13% trypsin (Invitrogen, Carlsbad, CA, USA), 0.01% papain (Invitrogen) and 0.01% DNase (Invitrogen) in a 37°C water bath for 7 minutes. An equal volume of trypsin inhibitor (Invitrogen) was added and the tissue was dispersed into a single cell suspension. The cells were centrifuged at 700 r/min for 7 minutes, resuspended in serum-free medium and washed twice. Live cells were quantified by benzo blue staining and the cell survival rate was greater than 95%. Cells were cultured in 25 mL culture bottles at a concentration of 1×10^6/mL. Cells were cultured in Dulbecco's Modified Eagle's medium/F12 (Invitrogen) containing NeuroCult NS-A proliferation supplement (Stem Cell Technology, Boston, CA, USA), 0.02% bovine serum albumin (Sigma-Aldrich), epidermal growth factor (Chemicon, Temecula, CA, USA) at a final concentration of 20 ng/mL, 10 ng/mL basic fibroblast growth factor and 0.002% heparin (Stem Cell Technology)[25] at 37°C, 5% CO_2. Half of the medium was exchanged every 3 or 4 days according to the color of medium and the state of the cells. Cells were passaged mechanically every 7 days.

BrdU (Sigma-Aldrich) was added to the culture medium at a final concentration of 10 μmol/L and the cells were labeled for 24 hours at 37°C and 5% CO_2. The primary antibodies were rabbit anti-nestin polyclonal antibody (1:500; Sigma-Aldrich) and mouse anti-BrdU polyclonal antibody (1:100; Sigma-Aldrich). Cells were incubated with secondary goat anti-rabbit IgG (1:100; Sigma-Aldrich) labeled with rhodamine and goat anti-mouse IgG (1:100; Sigma-Aldrich) labeled with fluorescein isothiocyanate for 2 hours at 37°C. The double-labeled cells were observed by fluorescence microscopy (PMTVC IC 05195, Olympus, Tokyo, Japan).

Detection of survival of neural stem cells in the tissue-engineered nanometer scaffolds using the MTS assay

96-well plates were randomly divided into a control group, an aligned group, and a random group, with eight wells in each group. Nanofiber membranes were disinfected by ultraviolet irradiation for 12 hours, swelled with culture medium, cut into strips and placed into the bottom of the wells. Cells were plated at a concentration of 1×10^5/mL in the 96-well plates, 100 μL per well. After 1, 3, 5, 7 and 9 days of incubation, cell proliferation was determined using the MTS assay (Cell Titre 96 "AQueous One Solution" Promega, Madison, WI, USA). Four plates were used at each time point. The MTS reduction was used as an indicator of viable cell number and was widely employed to examine cell proliferation. Briefly, each well was treated with 20 μL of AQueous One Solution and incubated at 37°C with 5% CO_2 for 2 hours. Blank wells were filled with culture medium and formazan dye. Absorbance values were read at 490 nm using a microplate reader (Multiskan MK3, Wisdom Scientific Instrument Co., Ltd., Shanghai, China). The quantity of formazan product (absorbance value) was directly proportional to the number of metabolically active living cells.

Determination of cell proliferation and apoptosis using flow cytometry

Culture bottles were randomly divided into a control group, an aligned group and a random group with six bottles in each group. Nanofiber membranes were disinfected by ultraviolet irradiation for 12 hours, swelled with culture medium, cut into strips and placed into the bottom of the bottles. The cells were then plated at a concentration of 4×10^5/mL. Cells were cultured in the bottles for 7 days. (1) Cell cycle assay: cells were fixed with ice-cold 70% ethanol and washed with PBS (pH 7.4). Cells were centrifuged and residual PBS was discarded. The cells were then resuspended in 300 mL propidium iodide solution (69 mmol/L in Na-citrate) (Sigma-Aldrich) plus 100 mg/mL RNase (Invitrogen). The cells were incubated at 37°C for 1 hour and analyzed on a FACSCalibur flow cytometer (Becton Dickinson, Sunnyvale, CA, USA). Data were collected using fluorescent activated cell sorting Diva software (Becton Dickinson). Tests were repeated four times. (2) Apoptosis assay: cells were fixed with ice-cold 70% ethanol and washed with PBS (pH 7.4). Cells were centrifuged and residual PBS was discarded. RNase (Invitrogen) was added to a final concentration of 60 μg/mL and incubated for 30 minutes. Propidium iodide (Sigma-Aldrich) was added to a final concentration of 50 μg/mL and incubated for 30 minutes at 4°C in the dark. Total cellular DNA content analysis and normal cells or apoptotic cells were distinguished by flow cytometry. Tests were repeated four times.

Analysis of cell differentiation by flow cytometry

Cell grouping and treatment were the same as described above. Cells were treated with induction medium comprising Dulbecco's Modified Eagle's medium/F12 (Invitrogen) and 1% fetal bovine serum (Sigma-Aldrich) for 1 week. Cells were trypsinized and prepared as a

single cell suspension. The cells were fixed in –20°C cold 70% ethanol/50 mmol/L glycine buffer (pH 2.0) for 20 minutes, and then washed with PBS. Cells were then incubated with a monoclonal antibody against microtubule-associated protein 2 (Sigma-Aldrich) followed by a fluorescein isothiocyanate-conjugated secondary antibody (Sigma-Aldrich), and then subjected to flow cytometry. Data were collected using appropriate electronic gating to remove background debris and aggregates. Microtubule-associated protein 2-positive cell ratio[26] was used to calculate the rate of differentiation of neural stem cells into neurons.

Analysis of gene expression by real-time quantitative PCR

Cells were trypsinized and prepared as a single cell suspension following culture on nanofiber membranes. The total RNA was extracted using Trizol RNA extraction agent (Sigma-Aldrich) according to the manufacturer's instructions. The extracted RNA was reverse-transcribed to cDNA using M-MLV reverse transcriptase and amplified by PCR using the following primers:

Primer	Sequence	Product length (bp)
GAPDH	Upstream primer: 5′-ATC CTG CAC CAC CAA CTG CT-3′ Downstream primer: 5′-GGG CCA TCC ACA GTC TTC TG-3′	110
HPRT	Upstream primer: 5′-TTC TTT GCT GAC CTG CTG GA-3′ Downstream primer: 5′-CCC CGT TGA CTG GTC ATT ACA-3′	110
Bax	Upstream primer: 5′-GTG GTT GCC CTC TTC TAC TTT GC-3′ Downstream primer: 5′-GAG GAC TCC AGC CAC AAA GAT G-3′	110
Bcl-2	Upstream primer: 5′-CTG GGA TGC CTT TGT GGA ACT-3′ Downstream primer: 5′-CCA GGT ATG CAC CCA GAG TGA-3′	110
Caspase-3	Upstream primer: 5′-TAA GGA AGA TCA CAG CAA AAG G-3′ Downstream primer: 5′-TGA GCA TTG ACA CAA TAC ACG-3′	110
Cyclin D1	Upstream primer: 5′- GGA GTG TGG TGG CCG CGA TG-3′ Downstream primer: 5′-CGG AGG CAG TCC GGG TCA CA-3′	110
CDK2	Upstream primer: 5′-TCT CAC CGT GTC CTG CAC CGA-3′ Downstream primer: 5′-GGC CCT GCG GGT CAC CAT TTC-3′	110

HPRT: Hypoxanthine guanine phosphoribosyl transferase; CDK2: cyclin-dependent kinase 2.

PCR reaction system: 5 μL SYBR Green PCR Master Mix (Roche), 3 μL cDNA, 0.15 μL (1 μmol/L) upstream primer, 0.15 μL (1 μmol/L) downstream primer in a total volume of 11 μL. Quantitative PCR reactions were performed as follows: a denaturation step of 95°C for 10 minutes, and then 40 cycles of amplification at 95°C for 15 seconds and 60°C for 1 minute, followed by a melting curve program. Two housekeeping genes, GAPDH and hypoxanthine guanine phosphoribosyl transferase, were used as endogenous control/reference genes. The relative expression levels of the genes of interest were normalized to the mean of the two housekeeping genes. Relative expression of the target genes was analyzed with matching analysis software (Rotor-Gene Q, Los Angeles, CA, USA). The relative amount of target gene expression was calculated using the $2^{-\Delta\Delta t}$ method. Tests were repeated four times.

Statistical analysis

Data were analyzed using SPSS 16.0 software (SPSS, Chicago, IL, USA). Measurement data were expressed as mean ± SD, and one-way analysis of variance was used. A value of $P < 0.05$ was considered statistically significant.

Acknowledgments: We are grateful to all of the teachers at the Central Laboratory and Animal Center of the Second Hospital Affiliated to Harbin Medical University in China for their help with the experiments.

Author contributions: Meng Yao and Yansong Wang participated in the study design. Jihui Zhou, Fuge Sui and Yugang Liu performed the experiments. Jihui Zhou and Yansong Wang were responsible for data analysis. Jihui Zhou wrote the manuscript and performed the statistical analysis. Yansong Wang and Meng Yao participated in article authorization. Feipeng Tian, Xiaofeng He, Lin Shao, Zhiqiang Liu and Qiang Li were in charge of data access. All authors approved the final version of the paper.

Conflicts of interest: None declared.

Ethical approval: The experiments were approved by the Experimental Animal Care and Use Committee of Shanghai Institute of Materia Medica Affiliated to Chinese Academy of Sciences.

Author statements: The manuscript is original, has not been submitted to or is not under consideration by another publication, has not been previously published in any language or any form, including electronic, and contains no disclosure of confidential information or authorship/patent application disputations.

REFERENCES

[1] Hou TY, Wu YM, Zhang YB. Research progress in tissue-engineered spinal cord repairing spinal cord injuries. Zhonghua Chuangshang Zazhi. 2005;21(4):316-318.

[2] Jiang ZG, Li YH, Bi XB, et al. Application of biomaterials on spinal cord injury. Zhongshan Daxue Yanjiusheng Xuekan: Ziran Kexue Yixue Ban. 2007;28(2):20-25.
[3] Ellis-Behnke RG, Schneider GE. Peptide amphiphiles and porous biodegradable scaffolds for tissue regeneration in the brain and spinal cord. Methods Mol Biol. 2011;726: 259-281.
[4] Guo J, Su H, Zeng Y, et al. Reknitting the injured spinal cord by self-assembling peptide nanofiber scaffold. Nanomedicine. 2007;3(4):311-321.
[5] Batrakova EV, Li S, Vinogradov SV, et al. Mechanism of pluronic effect on P-glycoprotein efflux system in blood-brain barrier: contributions of energy depletion and membrane fluidization. J Pharmacol Exp Ther. 2001; 299(2):483-493.
[6] Kabanov AV, Batrakova EV, Alakhov VY. Pluronic block copolymers as novel polymer therapeutics for drug and gene delivery. J Control Release. 2002;82(2-3):189-212.
[7] Alakhov V, Klinski E, Lemieux P, et al. Block copolymeric biotransport carriers as versatile vehicles for drug delivery. Expert Opin Biol Ther. 2001;1(4):583-602.
[8] Prabhakaran MP, Ghasemi-Mobarakeh L, Ramakrishna S. Electrospun composite nanofibers for tissue regeneration. J Nanosci Nanotechnol. 2011;11(4):3039-3057.
[9] Xie J, MacEwan MR, Schwartz AG, et al. Electrospun nanofibers for neural tissue engineering. Nanoscale. 2010; 2(1):35-44.
[10] Christenson EM, Anseth KS, van den Beucken JJ, et al. Nanobiomaterial applications in orthopedics. J Orthop Res. 2007;25(1):11-22.
[11] Wang M, Zhai P, Chen X, et al. Bioengineered scaffolds for spinal cord repair. Tissue Eng Part B Rev. 2011;17(3): 177-194.
[12] Madigan NN, McMahon S, O'Brien T, et al. Current tissue engineering and novel therapeutic approaches to axonal regeneration following spinal cord injury using polymer scaffolds. Respir Physiol Neurobiol. 2009;169(2):183-199.
[13] Patino MG, Neiders ME, Andreana S, et al. Collagen as an implantable material in medicine and dentistry. J Oral Implantol. 2002;28(5):220-225.
[14] Madaghiele M, Sannino A, Yannas IV, et al. Collagen-based matrices with axially oriented pores. J Biomed Mater Res A. 2008;85(3):757-767.
[15] Subramanian A, Krishnan UM, Sethuraman S. Development of biomaterial scaffold for nerve tissue engineering: Biomaterial mediated neural regeneration. J Biomed Sci. 2009;16:108.
[16] Sparrey CJ, Choo AM, Liu J, et al. The distribution of tissue damage in the spinal cord is influenced by the contusion velocity. Spine (Phila Pa 1976). 2008;33(22): E812-819.
[17] Kroeker SG, Morley PL, Jones CF, et al. The development of an improved physical surrogate model of the human spinal cord--tension and transverse compression. J Biomech. 2009;42(7):878-883.
[18] van den Heuvel S. Cell-cycle regulation. WormBook. 2005:1-16.
[19] Martinou JC, Youle RJ. Mitochondria in apoptosis: Bcl-2 family members and mitochondrial dynamics. Dev Cell. 2011;21(1):92-101.
[20] Ishikawa T, Watanabe N, Nagano M, et al. Bax inhibitor-1: a highly conserved endoplasmic reticulum-resident cell death suppressor. Cell Death Differ. 2011;18(8): 1271-1278.
[21] Miao EA, Rajan JV, Aderem A. Caspase-1-induced pyroptotic cell death. Immunol Rev. 2011;243(1):206-214.
[22] Hu YY, Zheng MH, Cheng G, et al. Notch signaling contributes to the maintenance of both normal neural stem cells and patient-derived glioma stem cells. BMC Cancer. 2011;11:82.
[23] The Ministry of Science and Technology of the People's Republic of China. Guidance Suggestions for the Care and Use of Laboratory Animals. 2006-09-30.
[24] Keyes-Baig C, Duhamel J, Fung SY, et al. Self-assembling peptide as a potential carrier of hydrophobic compounds. J Am Chem Soc. 2004;126(24):7522-7532.
[25] Tzeng SF. Neural progenitors isolated from newborn rat spinal cords differentiate into neurons and astroglia. J Biomed Sci. 2002;9(1):10-16.
[26] Efthimiou P, Blanco M. Pathogenesis of neuropsychiatric systemic lupus erythematosus and potential biomarkers. Mod Rheumatol. 2009;19(5):457-468.

(Reviewed by Robens J, Pack M, He SM, Suo YF)
(Edited by Yu J, Qiu Y, Li CH, Song LP)